AAEC/E631

AUSTRALIAN ATOMIC ENERGY COMMISSION
RESEARCH ESTABLISHMENT
LUCAS HEIGHTS RESEARCH LABORATORIES

ANALYSIS OF HYPOTHETICAL LOSS-OF-CONTROL-ARM ACCIDENTS IN HIFAR

by

J.W. CONNOLLY
N. CLARK

NOVEMBER 1986

ISBN 0 642 59828 X

AUSTRALIAN ATOMIC ENERGY COMMISSION
RESEARCH ESTABLISHMENT
LUCAS HEIGHTS RESEARCH LABORATORIES

ANALYSIS OF HYPOTHETICAL LOSS-OF-CONTROL-ARM ACCIDENTS IN HIFAR

by

J.W. CONNOLLY
N. CLARK

ABSTRACT

The reactor power transient produced in the HIFAR materials testing reactor upon severance of a central coarse control arm connecting rod and the subsequent pivoting of the arm out of the core has been calculated for a range of reactor conditions likely to be encountered in normal operation. It is concluded that as long as the remaining arms of the control arm bank can be relied on to suppress the post power peak oscillations in power, the reactor will withstand the consequences of such an accident.

National Library of Australia card number and ISBN 0 642 59838 X

The following descriptors have been selected from the INIS Thesaurus to describe the subject content of this report for information retrieval purposes. For further details please refer to IAEA-INIS-12 (INIS: Manual for Indexing) and IAEA-INIS-13 (INIS: Thesaurus) published in Vienna by the International Atomic Energy Agency.

CONTROL ELEMENTS; DELAYED NEUTRONS; HIFAR REACTOR; PEAKS; POWER DISTRIBUTION; REACTIVITY; REACTIVITY COEFFICIENTS; REACTOR ACCIDENTS; REACTOR CORES; REACTOR SAFETY; TRANSIENTS

CONTENTS

1. INTRODUCTION

Control of excess reactivity in DIDO class reactors is achieved by means of six semaphore type control arm blades positioned between the rows of fuel elements, as shown in **figure 1**. The six arms are referred to as the coarse control arm (CCA) bank and serve a dual safety and control function. In the fully inserted position they are at an angle of 34° to the vertical, an angle which is conventionally referred to as the zero angular position 0°. Criticality can be achieved by movement of the complete bank between this angle and the conventional angle of 56°, at which the arms are in the horizontal position and exercise zero reactivity control.

Angular movement of the CCA bank is achieved by the vertical movement of a connecting rod attached to each arm, causing the arm to pivot about a fixed bearing. A consequence of this design is that failure of a connecting rod will allow an arm to swing freely through the normal 'full in' position of 0°, where reactivity control is at a maximum, to the vertical or -34° position, where the reactivity control is very small.

A characteristic of the reactivity transients induced by such CCA failures is that the early period of arm motion drives the reactor sub-critical. Protection against the following positive reactivity ramp is provided by a negative period trip which will release the remaining five arms and ensure safe reactor shutdown. Should this trip fail, or be delayed, the sequence of negative period — positive period allows the falling arm to attain a considerable velocity by the time that power level or positive period trips are actuated; that is, the reactor is already on a very short period when these trip relays open.

The AAEC's materials testing reactor HIFAR belongs to the DIDO class; the aim of previous safety assessments for this reactor [McCulloch and Corran 1968] was to determine the maximum reactivity that could be invested in a single CCA such that loss of this arm would not result in a transient fast enough to defeat the installed trip functions. These studies were conservative insofar as they neglected negative reactivity feedback produced by the energy released during a power transient and assumed steady-state limitations to the power producing coolant flow instabilities and thus burnout of the fuel elements.

Developments in reactor power transient analysis carried out at the AAEC Research Establishment during the 1970s [Clancy *et al.* 1975, 1976] have made it possible to calculate the power transients following the loss of a CCA blade from various critical angles, with the inclusion of reactivity feedback effects and with a detailed representation of the fuel element geometry. The results of these calculations and the conclusions drawn from them are the subject of this report.

2. DATA REQUIREMENTS FOR TRANSIENT ANALYSIS

The results of an analysis of a loss-of-control-arm accident depends crucially on two parameters — the reactivity gain following an arm swinging to the -34° position and the magnitude of the negative reactivity energy coefficients. The source of these data, and of data of lesser importance but required in the analysis, is discussed in the following subsections.

2.1 Coarse Control Arm Bank Reactivity Calibration

An important influence on the reactivity controlled by the CCA bank is the ^{235}U inventory in the core. Elementary perturbation theory suggests that the CCA bank worth should be inversely proportional to this core fuel loading (M_5). Examination of the calibration data of Connolly and McKenzie [1960] for two cores containing 2.87 and 2.5 kg of ^{235}U, respectively, led us to conclude that these data were best correlated by an $M_5^{-0.5}$ dependence of reactivity control on core mass. Harries [1978] deduced an exponent of -0.75 $\pm$ 0.1 from least-squares fitting to the results of inverse kinetics measurements of the differential worth of the CCA bank at different core loadings. More recently, Robinson [AAEC unpublished report] concluded, from three-dimensional diffusion theory calculations, that the exponent varied with CCA position, obtaining values of -0.508, -0.654 and -0.800 as averages in the value of the exponent in the angular position ranges of 56-25°, 25-18° and 18-13°, respectively. However, these calculations were not available at the time the transient analysis of the loss-of-CCA accident was undertaken, the value of -0.5 was assumed when correcting reactivity data to a common core inventory. Although it is now clear that the Harries data are to be preferred, it can be shown that the error introduced by using a smaller exponent is not significant over the relatively small range of M_5 examined here.

Reactivity calibrations of the CCAs for the DIDO class reactors HIFAR, FRJ-2 and DIDO*, obtained during their commissioning or subsequent operation, have been corrected to a common core mass of 2.8 kg by means of an

* DIDO reactor is sited at the UK Atomic Energy Research Establishment Harwell, and FRJ-2 is at KFK Julich in the Federal Republic of Germany.

$M_5^{-0.5}$ dependence and the results for the differential reactivity worth of the bank are shown in **figure 2.** The HIFAR data were obtained from doubling time measurements, the difference between the 1960 and 1972 data being attributed to the difference in the reactor absorber loading used to produce a given critical angle. The FRJ-2 curve was obtained from pulsed sub-critical techniques and the 1958 DIDO data from a combination of calibrated poison strips and doubling time measurements; the 1966 results were obtained with a reactivity meter.

Although it is apparent that the loading of the reactor may produce significant changes in the shape of the differential bank worth curve, the mass corrected integral worth at a given angle for the three reactors agrees quite well, as is shown in table 1.

TABLE 1
COMPARISON OF INTEGRAL BANK WORTHS

	Integral Worth $\delta k/k$				
CCA Angle	HIFAR 1960	HIFAR 1972	DIDO	FRJ-2	Mean
10 °	0.122	0.123	0.123	0.124	0.123
12 °	0.102	0.102	0.102	0.106	0.103
14 °	0.081	0.081	0.084	0.088	0.084
16 °	0.064	0.063	0.068	0.073	0.067

2.2 Reactivity Control of a Central Arm as a Function of Angle

Analysis of the loss-of-CCA accident requires that the variation of core reactiviy with the position of the broken arm be known. The only feasible measurements of this variation are for the case in which only the connecting rod fails and the arm swings about the pivot bearing to the vertical position.

A convenient integral parameter is the reactivity gain in moving an arm from the bank at the angle ψ to the angle 34°, divided by the reactivity control of the complete bank at the angle ψ. **Figure 3** shows the variation of this ratio with the angle ψ as measured by Fassbender *et al.* [1965] on FRJ-2, and by Connolly and McKenzie [1960] on HIFAR. Because at -34° the arm exercises a small but significant reactivity control, which may be greater than the total worth of the bank at very high angles, this curve must pass through zero and the ratio assume negative values for large values of ψ. (It is for this reason that the error on the HIFAR data point at 27° is so large, since the difference in reactivity between the case with the complete bank at 27° and that with arm No.2 at -34° and the remaining five arms at 27° was very small.)

More data are available for the gain in reactivity when an arm is raised to the horizontal (56°) position where, since the arm is above the level of the moderator in the reactor tank, the reactivity controlled is zero. **Figure 4** shows results obtained by Parsons [1960, AERE unpublished report], Connolly and McKenzie [1960], Connolly [1963, AAEC unpublished report] and Fassbender *et al.* [1965]. Quite good agreement is shown here for the data from the three reactors. The single HIFAR data point designated by "10^5 MWh irradiation" represents a measurement on an arm at the end of its life, when cadmium burnup has led to some loss of reactivity control.

To calculate the details of the power transient as the broken arm swings through the core, data are required on the reactivity controlled by the arm as a function of angular position. These data, derived from Connolly and McKenzie [1960], Connolly [1963] and Fassbender *et al.* [1965], are rather limited and are shown in **figure 5.** a reasonable 'universal' shape was found for the normalised reactivity as a function of angle, which was independant of the parking position of the remaining arms. This curve was assumed to pass through zero at an angle of -34° (a conservative assumption) and used in conjunction with figure 3 and the data of table 1 to determine the variation in reactivity with angle as the broken arm swings through the core. The total reactivity insertion obtained in this manner for three initial arm angles in a 2.9 kg ^{235}U core is shown in table 2.

TABLE 2
REACTIVITY GAIN ON LOSS OF CCA

Arm Falling from ψ to -34°	Reactivity Gain $\delta k/k$
10°	0.0219
12°	0.0191
14°	0.0151

2.3 Angular Dynamics of a Falling Coarse Control Arm

Following Meister and Kalker [1964], the equation of motion of an arm pivoting from the core is assumed to be that of a braked pendulum:

$$\ddot{\psi} + \omega^2 \sin(\psi + 34) - A\dot{\psi}^2 = 0 \quad , \tag{1}$$

in which $\ddot{\psi}$ and $\dot{\psi}$ are the angular acceleration and velocity, respectively, ω is the frequency of the oscillation, and A is a constant determined by the resistance of the D_2O to the angular motion (the braking constant).

The braking constant A was determined by forcing agreement between numerically computed drop times from an angle of 20° and the mean of twenty three measured drop times recorded for arm No.2 in HIFAR (378 ± 24 ms) from this angle. The value obtained (A = 4.0) gave quite good agreement (365 ms) with the mean experimental value and also with the arm position/time data measured by Marshall and Blevins [1983]. The arm motion for the case with A = 0 was also computed since it represents the physical limit to the angular velocity with which the arm can swing from the core.

In conjunction with the data given in section 2.2, these calculations enabled the preparation of tables of reactivity *v.* time following the postulated breaking of an arm connecting rod.

2.4 Prompt Neutron Lifetime

Because the excess reactivity following the loss of a control arm from the core is, in general, large, the value of the prompt neutron lifetime $(\ell)^*$ is important when determining the rate of change of reactor power. Fassbender *et al.* [1965] reported measurements of the ratio of effective delayed neutron fraction to prompt neutron lifetime, β_{eff}/ℓ^*, for four reactor configurations in FRJ-2, the mean value being 12.4 s^{-1}. From the value of β_{eff} of 6.96 × 10^{-3} quoted by these authors, a value of $\ell^* = 560 \pm \mu s$ is obtained.

Crick and Nicholson [1966] quoted a value of 460 μs, obtained from measurements on the DIDO mockup core DAPHNE; no error assignment was given. In 1982, Robinson and Harrington [AAEC unpublished report] calculated ℓ^* in XY and RZ geometries for high and low burnup cores; mean values for the two geometries were 583 and 529 μs for high and low burnup, respectively.

In the present work a value for ℓ^* of 500 μs is adopted; any lower value could only be produced by extensively poisoning the core, in which case the excess reactivity would be sufficiently small for the loss-of-control-arm accident to be of no real concern.

2.5 Effective Delayed Neutron Fraction

Fassbender *et al.* [1965], Crick and Nicholson [1966] and Duerden [1972, AAEC unpublished report], gave values for β_{eff} of 6.96, 6.68 and 7.04 × 10^{-3}, respectively. These are believed to contain the contribution from photoneutrons. The 1982 value calculated by Robinson and Harrington for both high and low burnup cores was 6.9 × 10^{-3}, excluding the photoneutron contribution. For the calculations made in the present report, the value of β_{eff} was taken as 7 × 10^{-3}.

2.6 Reactivity Feedback Coefficients

For power transients in which the reactor period is short compared with the transit time of the coolant through the core, the dominant source of reactivity feedback comes from energy deposited in the coolant at about the time of peak power. To calculate this feedback, the values of the coolant temperature coefficient of reactivity at constant coolant density and the coolant density coefficient of reactivity at constant temperature are required. Experimental information on the magnitude of these two coefficients is meagre, so it has been necessary to obtain them from two-dimensional diffusion theory calculations. From these calculated values, the total coolant temperature coefficients of reactivity shown in table 3 have been derived and used in the transient calculations reported here.

TABLE 3
COOLANT TEMPERATURE COEFFICIENTS OF REACTIVITY

Coolant Temperature θ (°C)	$1/k.(\delta k/d\theta \times 10^5)$
20	-10.3
40	12.0
50	-14.5

As a check on the calculational procedures used to generate the data of table 3, a comparison has been made of the calculated and experimental values of the whole reactor (coolant, moderator and reflector) isothermal temperature coefficient for the DIDO class reactors DIDO, HIFAR, FRJ-2 and DR-3*; the results are shown in figure 6.

The experimental results for HIFAR and DR-3 are in good agreement with calculation in both magnitude and the dependence on temperature. The temperature dependence for the 1965 DIDO and the FRJ-2 results shows the same trend as the calculation but the absolute magnitude of the reactivity coefficient at 40°C is lower by 20 and 30 per cent, respectively. The 1966 DIDO data bear no resemblance to the calculated data nor indeed to those measured earlier on this reactor. Unfortunately, insufficient information on the conditions under which these measurements were made is given in the reports from which the data were obtained, so further analysis is not possible.

If the 1966 DIDO results are taken as anomalous and discarded, the mean of the experimental data at 40° gives a coefficient of -40×10^{-5} $\delta k/k$ per °C compared with the calculated value of -46×10^{-5} $\delta k/k$ per °C; an estimate of the accuracy of the data of table 3 might then be taken as -15 per cent. However, identical calculational procedures for obtaining coolant reactivity coefficients for the DIDO type SPERT core BD22/24 [Connolly 1982] enabled power burst parameters to be calculated that were in agreement with experimental values to better than 10 per cent; this is a more realistic estimate of the errors associated with the data of table 3.

2.7 Material Properties

Temperature-dependent thermal properties of fuel alloy and aluminium clad used in the present calculations have been taken from Houghtaling *et al.* [1964]. The temperature dependence of the D_2O density comes from data given by Turner [1968].

3. TRANSIENT ANALYSIS

The code ZAPP [Clancy 1982] solves the reactor kinetic equations which, with the usual symbols, are

$$\frac{dn}{dt} = \left\{ \frac{k(t).(1-\beta) - 1}{\ell^*} \right\} n + \sum_i \lambda_i C_i \quad , \tag{2}$$

$$\frac{dC_i}{dt} = \frac{k(t)\beta_i n}{\ell^*} - \lambda_i C_i \quad , \tag{3}$$

with a coupling equation between the time-dependent multiplication factor k(t) and the temperature distribution in a cell consisting of fuel alloy, clad and coolant given by the one-dimensional heat transfer equation

$$c(\theta,x) \frac{\partial}{\partial t}\left[\theta(x,t)\right] = \frac{\partial}{\partial x}\left[K(\theta,x) \frac{\partial}{\partial x} \theta(x,t)\right] + S(x,t) \quad , \tag{4}$$

and

$$k(t) = k_o + \int_o^L dx \int_{\theta_o}^{\theta(x,t)} \frac{dk}{d\theta}(x,\theta)\, d\theta \quad , \tag{5}$$

where c is the specific heat/unit volume, θ is the temperature, K is the thermal conductivity, S is the heat source, L is the width of the cell, and $\delta k/d\theta$ is the temperature coefficient of reactivity/unit volume.

The novelty introduced by the use of ZAPP to calculate reactor power transients lies in the method of modelling nucleate boiling heat transfer. A more detailed description was given by Connolly [1977] but, in essence, the method adopted is to divide the coolant channel into a number of very small regions and allow the thermal conductivity of these regions to become large when a trigger temperature is reached. The model produces the

* The DR-3 reactor is sited at Riso, Denmark.

breakdown of the near exponential spatial distribution of temperature established in the coolant before the onset of nucleate boiling and its replacement by a near isothermal temperature front propagating away from the clad/coolant interface. This modelling of nucleate boiling heat transfer has given excellent agreement between data measured on a variety of SPERT cores [Clancy *et al.* 1975, 1976; Connolly and Harrington 1977] for all transients in which steam void generation was not a dominant shutdown mechanism.

An empirical model of steam void formation in the coolant channels was determined by forcing agreement between ZAPP calculation and experiment for the SPERT core BD22/24 subjected to a transient of initial period 50 ms. The parameters adjusted to attain agreement with the measured energy release at the time of peak power were the temperature of the superheated coolant layer at which steam bubbles, and hence void, commenced to grow, and the linear rate at which void growth decreased the density of the superheated coolant layer. The parameters thus determined were then used to calculate the contribution of steam void to reactor shutdown in the HIFAR loss-of-control-arm accident.

4. LOSS OF COARSE CONTROL ARM TRANSIENT ANALYSIS

From the data given in section 2.2, the transient caused by a central control arm pivoting from the core has been calculated for initial critical angles (the angular position of the bank required to maintain a constant reactor power) of 10, 12 and 14°. The variation of reactivity with position of the falling arm was represented as a series of constant ramp rates between angular positions at intervals of two degrees which, when changed to a time variable produced the ramp rate *v.* time data of **figure** 7. The use of an interrupt option in ZAPP enabled the data to be entered in the calculations at the appropriate times during the transient.

Although a simple coolant flow model is available in ZAPP, the detailed representation of the Mark IV fuel element geometry could not be retained if axial representation of the core, necessary in the flow model, was used. Since Connolly and Harrington [1977] had shown by calculation and Johnson *et al.* [1965] by experiment that the values of peak power and energy release in severe transients were insensitive to the magnitude of the flow rate because of the rapid rate of feedback, the zero flow model was retained in the analysis of the loss-of-control-arm accident.

Power transients following the loss of a central arm were calculated for two reactor power levels at the time of arm failure, 10 kW and 10 MW, for each of the three critical angles above. In the case of an initial power of 10 MW, the calculations were run with A=0, corresponding to free fall and resisted fall (A=4.0). In addition, calculations with smaller values of the prompt neutron lifetime and initial moderator temperature were performed to assess the sensitivity of transient behaviour to these parameters.

Figure 8 shows typical results of calculations for an initial reactor power of 10 MW, three critical angles (10,12,14°) and braked and unbraked arm motion. The power data for transients from a critical angle of 10° were digitised and used to generate a current input into standard HIFAR power, doubling time and halving time trip units to obtain the time-to- trip response for such input signals. The details of this procedure are described in appendix A.

In the following subsections, detailed results of the calculations are given and discussed; in them the following nomenclature is used:

ψ_c	the critical angle at the time of arm failure.
P_{max}	the maximum reactor power attained during the transient.
E_{tm}	the energy release in the transient at the time of P_{max}.
E_{ti}-E_{fi}	the energy release in the time interval between the reactor power passing the steady-state flow instability power, and reaching P_{max}.
R_c	the rate of negative reactivity feedback at the time of P_{max}.
θ_{max}	the maximum fuel plate temperature attained.
α_{max}	the maximum inverse period attained.

4.1 Resistance to the Motion of the Falling Arm

Comparison of transient parameters calculated for an initial power of 10 MW and two values of the braking constant are shown in table 4. In this table the data given are for the case in which it is assumed that no shutdown action is provided by the remaining arms of the CCA bank. It is apparent from table 4 that although the

value of P_{max} is strongly dependent on the value of A, the most important parameters, E_{tm} and θ_{max}, are much less so. This is because the higher peak powers enhance the feedback which is non-linear with energy release from nucleate boiling and steam void formation, resulting in much sharper power pulse shapes and consequent smaller increases in energy release and temperature for the smaller value of A than is the case for P_{max}.

TABLE 4
CALCULATED TRANSIENT PARAMETERS WITH AND WITHOUT RESISTANCE TO ARM MOTION

A	ψ (°)	P_{max} (MW)	E_{tm} (MJ)	E_{tm}-E_{fi} (MJ)	R_c ($\frac{\delta k}{k}$ s^{-1})	θ_{max} (°C)	α_{max} (s^{-1})
4	10	205	18.1	13.5	-0.25	231	18.5
0	10	347	19.8	16.4	-0.49	267	29.0
4	12	151	16.2	11.3	-0.15	195	14.7
0	12	262	17.3	13.8	-0.34	233	25.0
4	14	107	15.3	9.7	-0.13	176	11.1
0	14	165	15.0	11.2	-0.18	198	19.0

The rates at which reactivity feedback is injected into the core R_c are all large and comparable to the rates at which the CCA bank can provide shutdown. Thus without actuation of a reactor trip, the transient behaves in a similar fashion to a transient with a trip initiated at a power corresponding to P_{max}. However, reactivity feedback cannot provide such a large and permanent reduction in core reactivity as the CCA bank. This is discussed in section 5.

4.2 Prompt Neutron Lifetime

The effect of varying the prompt neutron lifetime ℓ^* has been determined by calculating transients with values of ℓ^* of 300 and 500 μs, respectively, and with the common conditions that ψ is 10°, A is 4.0, the initial coolant temperature 20°C and the initial power is 10 MW; the results are given in table 5. It is clear that the prompt neutron lifetime is of small importance in determining the value of θ_{max} for any reasonable value of this parameter; the explanation is the same as that advanced to explain the weak dependence of θ_{max} on A in the preceeding section.

TABLE 5
INFLUENCE OF THE PROMPT NEUTRON LIFETIME ON TRANSIENT PARAMETERS

ℓ^* (μs)	P_{max} (MW)	E_{tm} (MJ)	R_c $\delta k/k$ s^{-1}	θ_{max} (°C)
300	323	18.6	-0.45	282
500	250	20.3	-0.27	263

4.3 Initial Coolant Temperature

Because of the temperature dependence of the reactivity feedback coefficients and the increased energy release to reach the thresholds for nucleate boiling and steam void formation, it might be expected that lowering the reactor coolant temperature at the onset of the transient would lead to larger values of P_{max} and E_{tm}. This is supported in table 6 where calculated transient properties are shown for two values of initial coolant temperature, 20 and 50°C. (Both transients have the common parameters $\ell^* = 500$ μs, A = 4.0 and initial power 10 MW.) The dependence of the transient on initial temperature, although interesting, is of no significance with respect to safety under transient conditions.

TABLE 6
TRANSIENT PARAMETERS FOR TWO INITIAL COOLANT TEMPERATURES

θ_{in} (°C)	P_{max} (MW)	E_{tm} (MJ)	θ_{max} (°C)
20	250	20.3	265
50	205	18.1	232

4.4 Initial Reactor Power

If the reactor power is sufficiently low at the time of control arm failure, the positive reactivity will be inserted before any reactivity feedback is generated and the reactor will respond as though the reactivity was added as a step change in reactivity. Table 7 gives transient parameters calculated for loss of an arm from 10°, an initial coolant temperature of 20°C, A = 4.0 and two values of the initial power, 10 kW and 10 MW. Also shown are the measured burst parameters on the SPERT II core BD22/24 for a step insertion of 0.02 δk/k, which is close to the 0.022 δk/k, inserted by the loss of an arm from 10°.

TABLE 7
COMPARISON BETWEEN TRANSIENT PARAMETERS IN HIFAR FOR TWO VALUES OF INITIAL POWER AND THOSE MEASURED IN SPERT II FOR A COMPARABLE STEP INSERTION OF REACTIVITY

Initial Power (P_{max}) (MW)	(E_{tm}) (MJ)	(E_{tm}-E_{ti}) (MJ)	(R_c) ($\frac{\delta k}{k}$ s^{-1})	(θ_{max}) (°C)	(α_{max}) (s^{-1})
455	22.8	21.4 22.6[a]	0.56	368	29
250	20.3	15.7	0.27	265	20
300	20.0	-	-	330	20
0.01 0.0001[b]					

(a) Assuming the reactor is in the low power mode, flow instability power 5MW.
(b) SPERT II BD22/24.

It can be seen from tables 5,6 and 7 that, if the reactor safety system fails to function, the loss of an arm with the reactor at low power produces the most severe transient. The maximum fuel temperature calculated for this transient is comparable to that produced in core BD22/24 for a similar reactivity injection.

4.5 Shutdown by the Remaining Arms of the CCA Bank

The results given in the preceding sections have only considered events to the time shortly after the first power peak because the validity of the no-coolant flow model is restricted to this range. With coolant flow, as shown by the SPERT II experiments, the post peak power behaviour will exhibit damped oscillations and approach an equilibrium power determined by the flow rate and the reactivity energy coefficient. A simple model incorporating these two parameters gives good agreement with SPERT II data, as is shown in table 8.

TABLE 8
COMPARISON OF MEASURED AND CALCULATED EQUILIBRIUM POWERS FOR SPERT II B18/68

Flow Velocity ($m\ s^{-1}$)	Equilibrium Power(calc.) (MW)	Equilibrium Power(exp.) (MW)
4.0	264	240
2.0	130	140
1.0	65	65
0.5	49	49

For HIFAR, the calculated equilibrium power following loss of an arm from 10° is 80 MW, which is well above the flow instability power (40 MW). Thus the details of the post peak power behaviour are not important since shutdown by the remaining arms of the CCA bank must be achieved before fuel burnout results from coolant flow redistribution in the core.

Following the procedures given in appendix A, the times taken for halving time (HT), doubling time (DT) and power level (PT) trip relays to open after following the loss of an arm from 10° have been determined. These are shown in figure 8 for an initial reactor power level of 10 MW and figure 9 for an initial power level of 10 kW. It can be readily seen that if the halving time trip functions, then the loss-of-arm accident is trivial.

From these figures, it can be seen that the order in which the trip relays open is reversed in each case. The time intervals between the trip relays opening and the attainment of peak power are shown in table 9. The reversal of the trip order occurs because the low power trip is set at 150 kW, which is much greater than the assumed initial power level of 10 kW; in the case of high power operation, the trip setting is only ten per cent above the operating power.

TABLE 9
TIME INTERVAL BETWEEN TRIP RELAYS OPENING AND REACTOR POWER REACHING P_{max}, ASSUMING CCA BANK FAILS TO DROP

Power (MW)	Trip Function	Time between Trip Relay Opening and Time of P_{max}
0.01	Doubling time	338
0.01	Power level	248
10.0	Doubling time	80
10.0	Power level	180

Connolly [1985, AAEC unpublished report] has shown that the delay between trip relays opening and the CCA bank commencing to fall is 113 ms at a confidence level of 95 per cent when the bank is initially at an angle of 10°. From table 9 it follows that it is only the doubling time trip for a transient initiated from a reactor power level of 10 MW which is inadequate to limit the transient to consequences less severe than those determined by reactivity feedback alone.

Figure 10 shows the calculated reactor power following loss of a central CCA from 10° and initial power of 10 MW, with four of the remaining five arms dropping into the core 100 ms after the power level trip relay opens. The peak power is 146 MW and the energy release at this time is 13.4 MJ. Shortly after peak power, the maximum fuel plate temperature of 188°C is reached. At 1.5 s after the start of the accident and with the four arms at the full in position, the power is 1.6 MW and the energy release since first passing the flow instability power is 18.8 MJ. (Insertion of the four arms to 0° has been assumed to add -0.054 δk/k to the reactor; this is a suitably conservative figure.)

5. DISCUSSION

The results of calculations given in the preceding sections have not considered the loss of an arm from a critical angle less than 10°. This is because the operational requirements of the reactor do not necessitate excess reactivities greater than 0.12 δk/k and, in most instances, are not greater than 0.1 δk/k. Thus, provided that the reactor is always operated within the mandatory limits governing core excess reactivity, the range of initial arm angles considered is satisfactory.

It has been shown that of the parameters entering the calculation of transients following a loss of an arm, all except the magnitude of the feedback coefficients, the initial reactor power and the total reactivity inserted by the falling arm exercise only a slight influence on the most important parameters, the energy release and the maximum fuel temperature.

Of these three exceptions, the reactor power is an unambiguous quantity, since it is known to probably better than ten per cent. The other criteria, however, have been inferred from measured and calculated data respectively and may be subject to random or systematic errors which are difficult to quantify. Fortunately, the shutdown mechanisms operating during these transients are highly non-linear with energy release, producing reactivity feedback with an $E^{1.8}$ dependence rather than $E^{1.0}$. It can be shown in the prompt neutron approximation applicable to these transients that the energy release should vary as

$$\left[\frac{\text{Excess prompt reactivity added to the core}}{\text{Energy coefficient of reactivity}}\right]^{\frac{1}{1.8}}$$

this prediction has been confirmed experimentally in the SPERT program for reactors, where the shutdown mechanisms have the general energy dependence of E^n and n varies from 1.0 to 2.0, depending on the type of reactor core.

Thus, in the case of the present calculations, if the actual reactivity released on the loss of an arm is 20 per cent greater and the reactivity coefficients 20 per cent smaller than assumed, the energy release would increase by the factor $(1.2/0.8)^{0.55}$ or 1.25. Since the calculated maximum temperatures are all much less than the melting point of aluminium (640°C), an increase in the energy release of this magnitude can be tolerated.

The possible influence of flow instability on transient behaviour remains to be discussed. This is a mechanism whereby the establishment of boiling at the coolant channel outlet alters the pressure drop across the channel in such a manner as to direct coolant flow into adjacent parallel channels. The steady-state power level marking the onset of flow instability in the highest rated fuel element in HIFAR has been calculated to be 40 MW, and safety studies usually assume (pessimistically) that beyond this power, flow instability causes dry-out of the channel and adiabatic heating of the fuel up to the melting point.

The calculations reported here have assumed that heat continues to be transferred from fuel to coolant at powers up to ten times greater than the flow instability steady-state power. This can be justified on the following grounds:

(i) The short timescale of the transients. Johnson *et al.* [1965] found that for SPERT II B18/68, it took several seconds to establish flow instabilities, burnout of the fuel elements occurring well after the first power peak.

(ii) Calculational procedure employed in this paper has yielded excellent agreement with transient parameters measured on the DIDO-type SPERT II core BD22/24. [Connolly 1982, AAEC unpublished report].

(iii) Transient powers required to produce boiling at the coolant channel outlets would clearly be considerably higher than the steady-state flow instability power if the rate of rise of the power in the transient is large, as is the case here.

These appear to be compelling reasons for accepting the validity of the calculated temperatures. However, because the core energy release required to raise the highest rated fuel element adiabatically to the melting point is 25 MJ, it can be seen from the values of E_{tm} - E_{ti} in tables 4 and 7 that it is only for the transient commencing from a low initial power that the energy released between passing the steady-state flow instability power and reaching P_{max} approaches the value of 25 MJ; under these very severe conditions, it should still be possible for the reactor safety system to terminate the transient safely if the data of table 3 are considered.

Although the calculated temperatures are well below the melting point of the fuel element, consideration must be given to the possible consequences of distortion of fuel element geometry as a consequence of thermal expansion. Direct information on the behaviour of fuel elements heated to high temperatures is limited, but it does not suggest that the temperatures calculated in this report are likely to produce severe deformation in fuel elements. Wolters [KFK Julich, private communication] found that a fuel element repeatedly raised to a temperature of 300°C suffered only minor out-of-round distortion of the fuel tubes and Panter [AERE, Harwell, private communication] considered that, in the PLUTO S2 fuel element, there was no incidental blockage of coolant channels from thermal distortion below a temperature of 550°C. The maximum fuel element temperature found in the present work is 368°C which, from the above evidence, is insufficient to produce serious distortion.

6. CONCLUSIONS

It has been found that HIFAR will withstand an injection of at least 0.022 δk/k at any rate physically attainable in a loss-of-CCA accident caused by severance of a control arm connecting rod. This conclusion may be extended to the case in which both the connecting rod and the pivot bearing fail, provided that the velocity with which the completely free arm falls from the core does not greatly exceed that attained during pendulum motion. This finding is qualified by the requirement that the remainder of the CCA bank shuts the reactor down in time to suppress the post power/peak power oscillations, but the time required to do this is long compared to actual delay times measured for the reactor safety system.

7. ACKNOWLEDGEMENTS

We wish to thank B.E. Clancy for continually updating ZAPP to cope with increasingly complex problems; we are also grateful to G. Robinson and B. Harrington for many nucleonic calculations.

8. REFERENCES

Clancy, B.E. [1982] - ZAPP - a computer program for the simulation of reactor power transients. AAEC/E568

Clancy, B.E., Connolly, J.W., Harrington, B.V. [1975] - An analysis of power transients observed in SPERT I reactors, Part I. AAEC/E345.

Clancy, B.E., Connolly, J.W., Harrington, B.V. [1976] - An analysis of power transients observed in SPERT I reactors, Part II. AAEC/E383.

Connolly, J.W. [1977] - A simple model of transient heat transfer and its application to power excursions in water-moderated nuclear reactors. *Second Australasian Conference on Heat and Mass Transfer*, Sydney.

Connolly, J.W. [1982] - The Venus syndrome. *DIDO Operators' Meeting*, Lucas Heights.

Connolly, J.W., Harrington, B.V. [1977] - An analysis of power transients observed in the SPERT II D_2O moderated close-packed core. AAEC/E418.

Connolly, J.W., McKenzie, C.D. [1960] - Reactor physics studies on the HIFAR twenty five fuel element cores. AAEC/TM64.

Crick, N.W., Nicholson, K.P. [1966] - Physics parameters and principles for the operation of DIDO at 15 MW. AERE-R5196.

Fassbender, J., Kramer, H., Meister, G. [1965] - Ergebnisse der Anfahrexperimente am Reaktor FRJ-2. Jul-236-RE.

Harries, J.R. [1978] - Inverse kinetics measurements on the materials testing reactor HIFAR. AAEC/E456.

Houghtaling, J.E., Sola, A., Spano, A. [1964] - Transient temperature distributions in the SPERT I D12/25 fuel plates. IDO-16884.

Johnson, R.L., Larson, H.A., McClure, J.A., Norberg, J.A. [1965] - An analysis of the excursion behaviour of a highly enriched plate type D_2O moderated core in SPERT II. IDO-17109.

McCulloch, D.B., Corran, E.R. [1968] - Analogue studies of power transients following loss of a single coarse control arm blade in the materials testing reactor HIFAR. AAEC/TM79.

Marshall, J., Blevins, R.J. [1983] - Measurements of coarse control arm drop characteristics in the materials testing reactor HIFAR. AAEC/E560.

Meister, H. and Kalker, K. [1964] - Analyse denkbarer Grobsteuerarm-Unfalle am Reaktor FRJ-2. Jul-146-RE.

Turner, W.J. [1968] - Calculation of SPERT transients. *J. Nucl. Eng.*, 22:397-409.

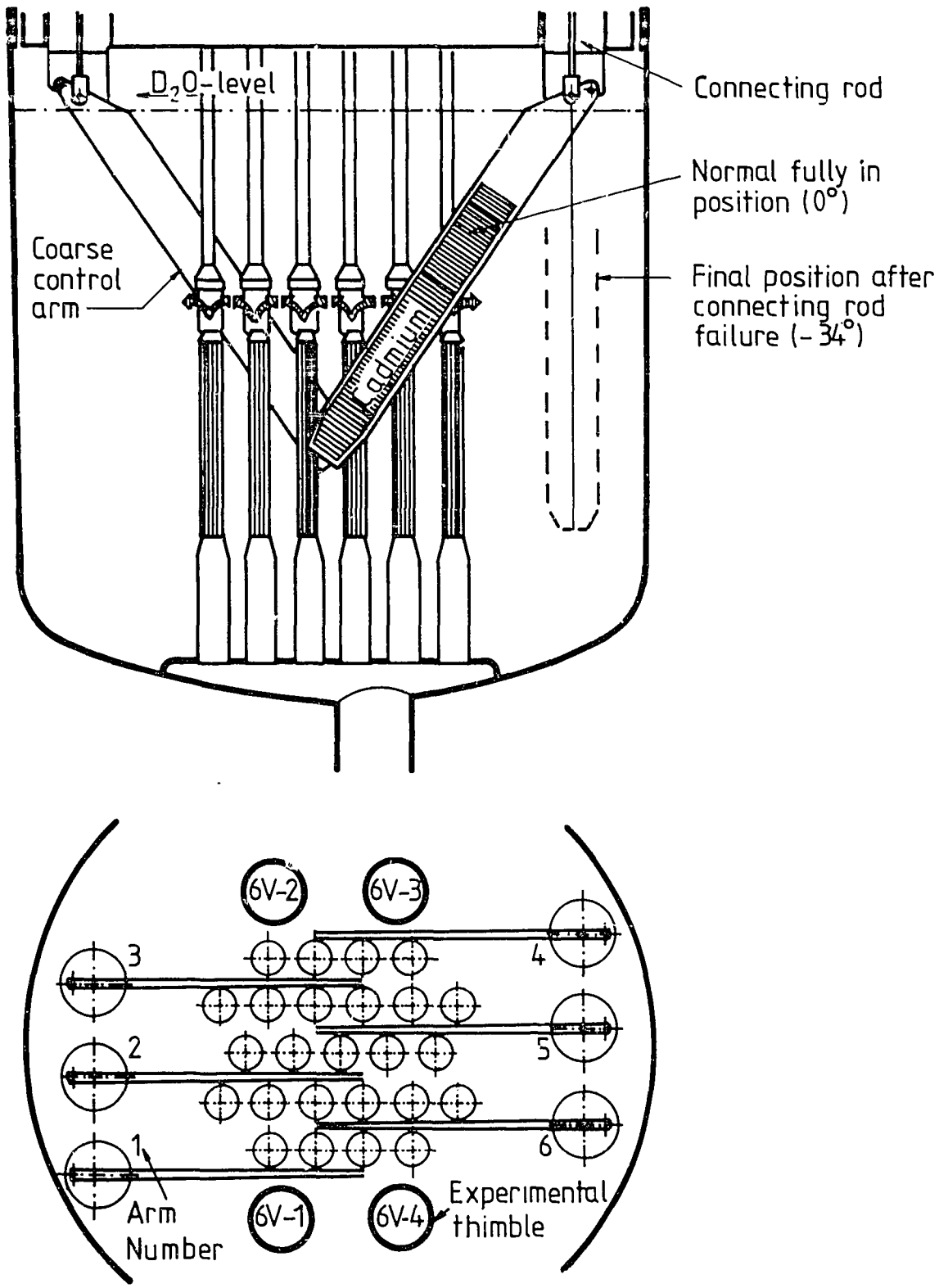

Figure 1 Elevation and plan view of coarse control arms (CCAs)

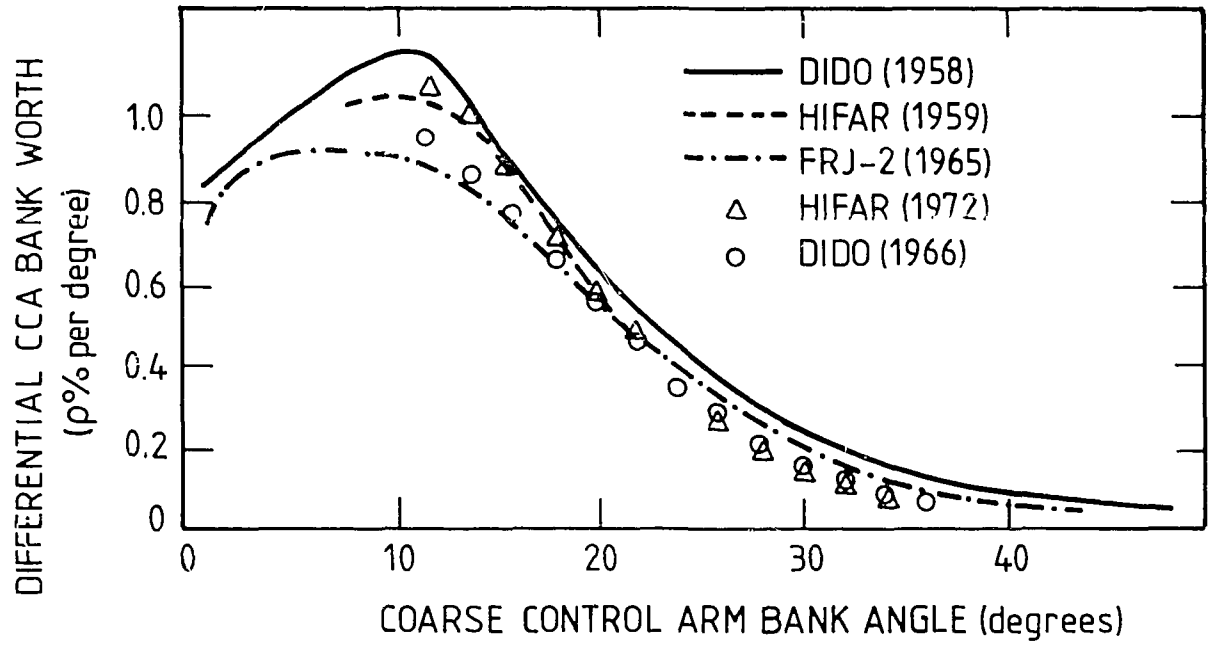

Figure 2 Comparison of differential control arm reactivity worths for three DIDO class reactors

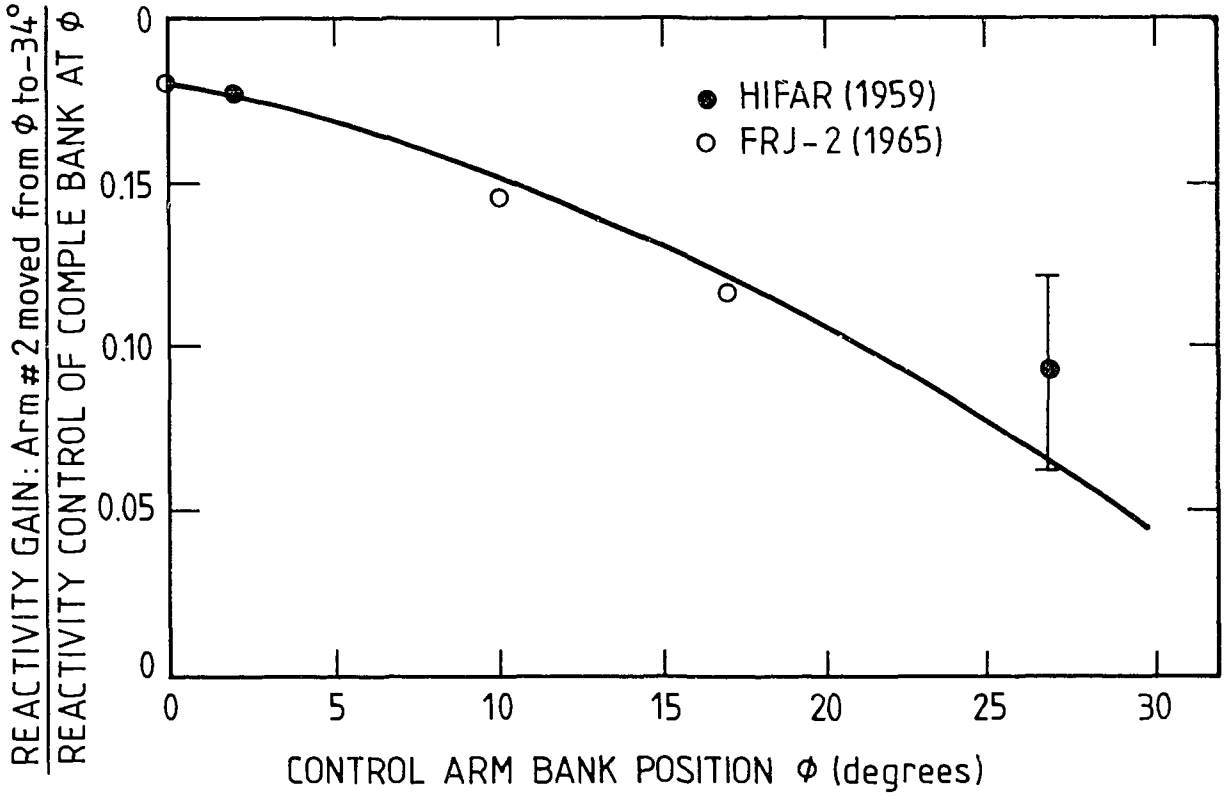

Figure 3 Ratio of the reactivity gained on moving a central CCA arm to the vertical position to the total CCA-bank worth as a function of CCA bank angular position

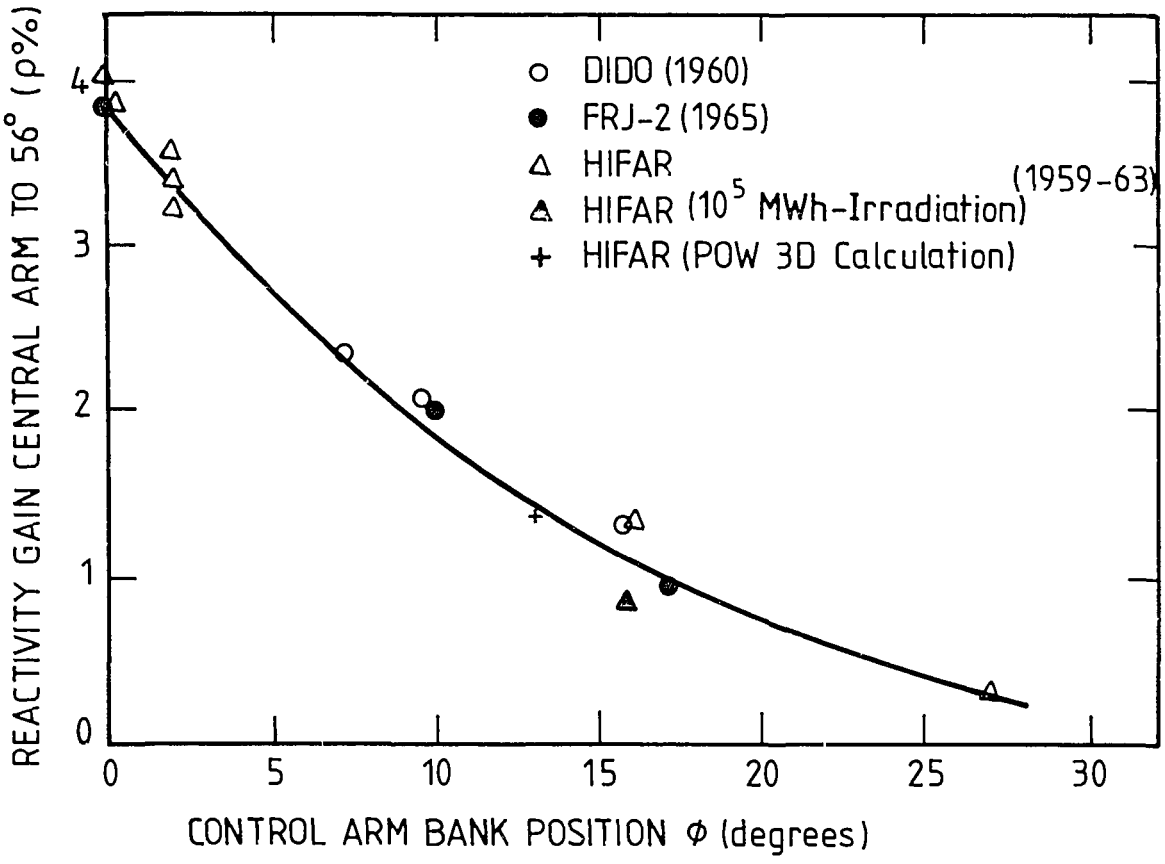

Figure 4 Reactivity gain following withdrawal of a central CCA to a horizontal position as a function of CCA-bank angle

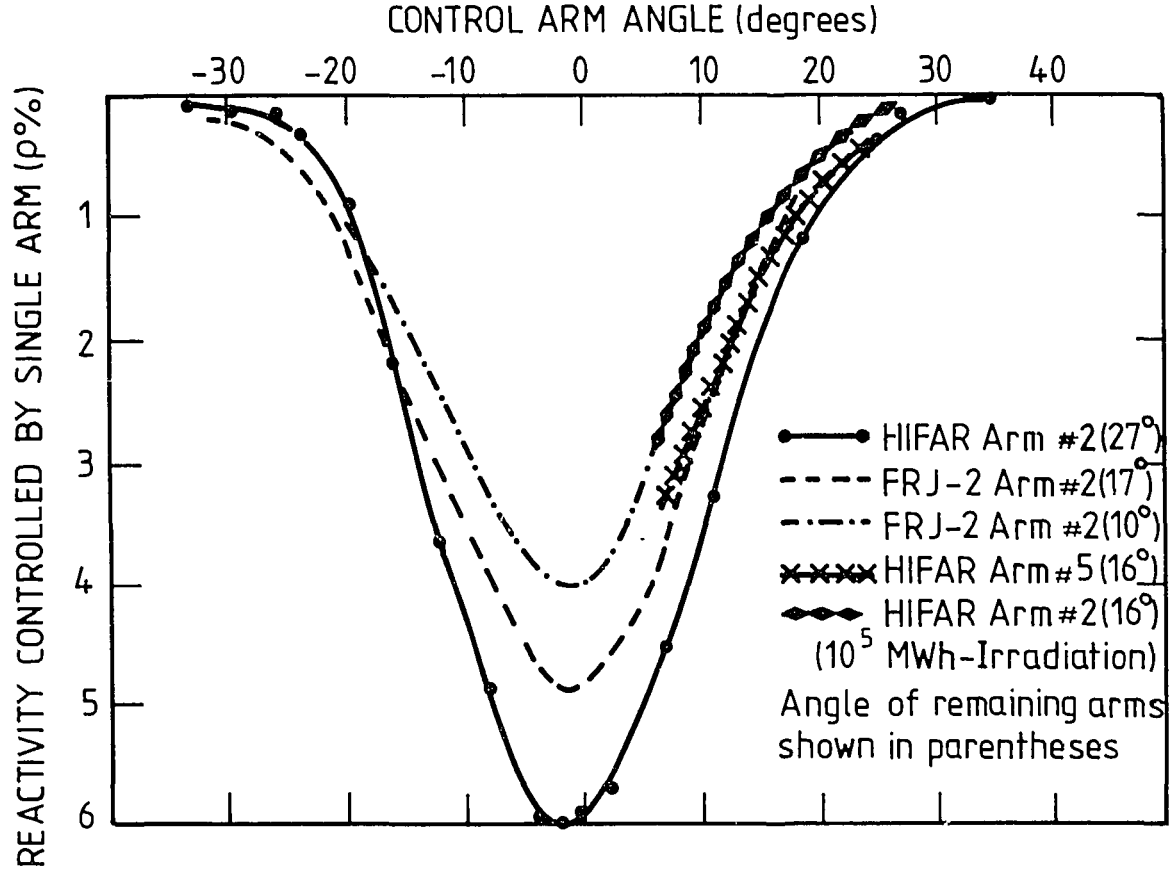

Figure 5 Variation of reactivity controlled by a single control arm as a function of angular position, with position of the remaining arms as a parameter

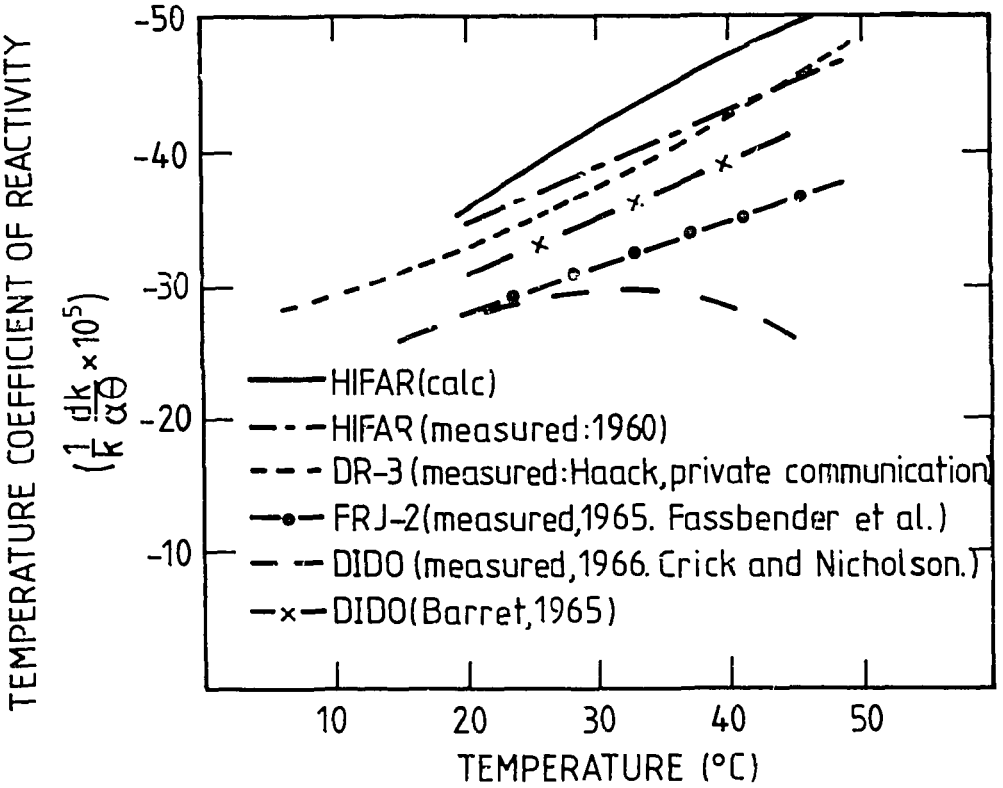

Figure 6 Whole reactor isothermal temperature coefficients for DIDO class reactors

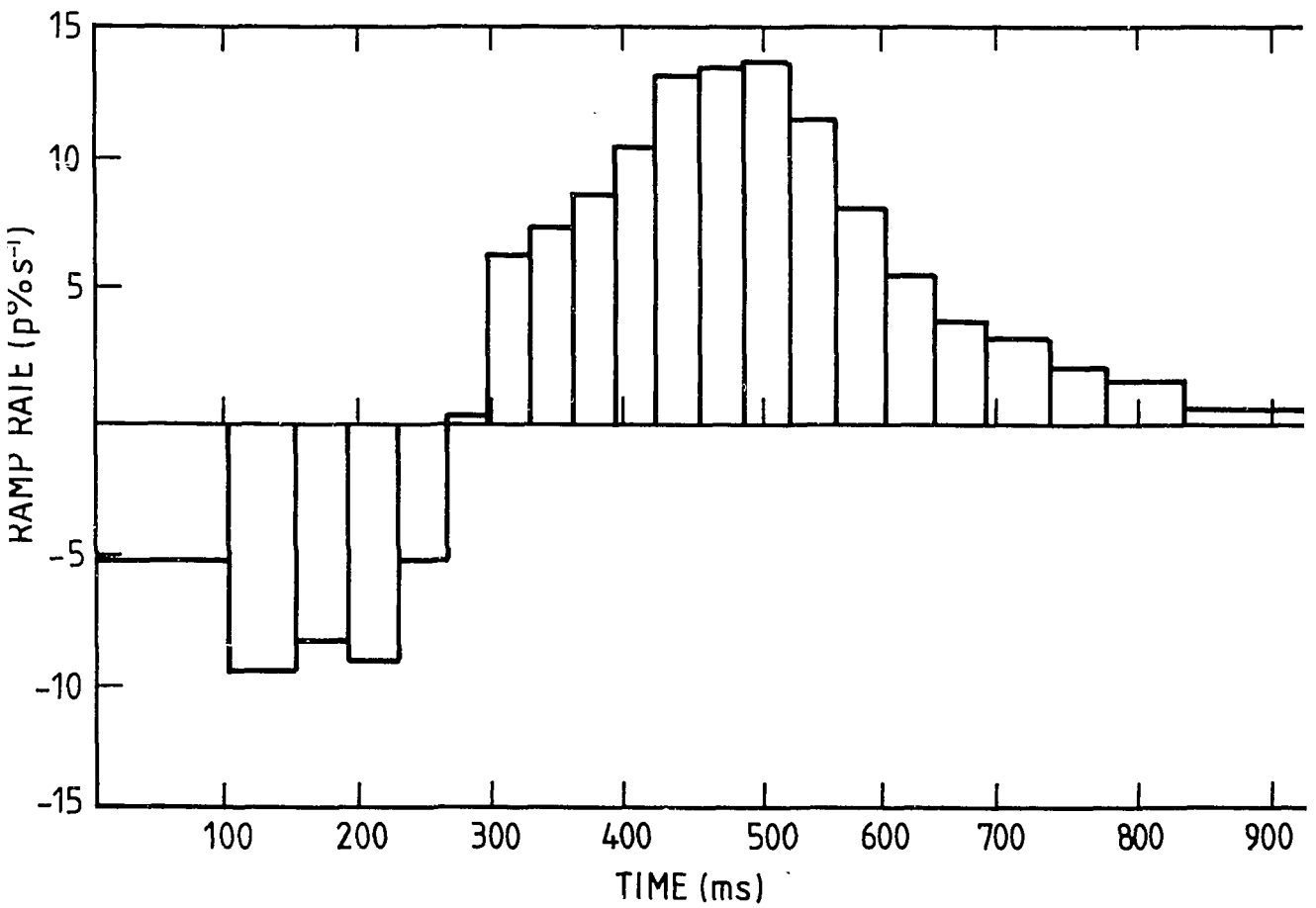

Figure 7 Representation of reactivity input function for loss of a central CCA at a critical angle of 10°

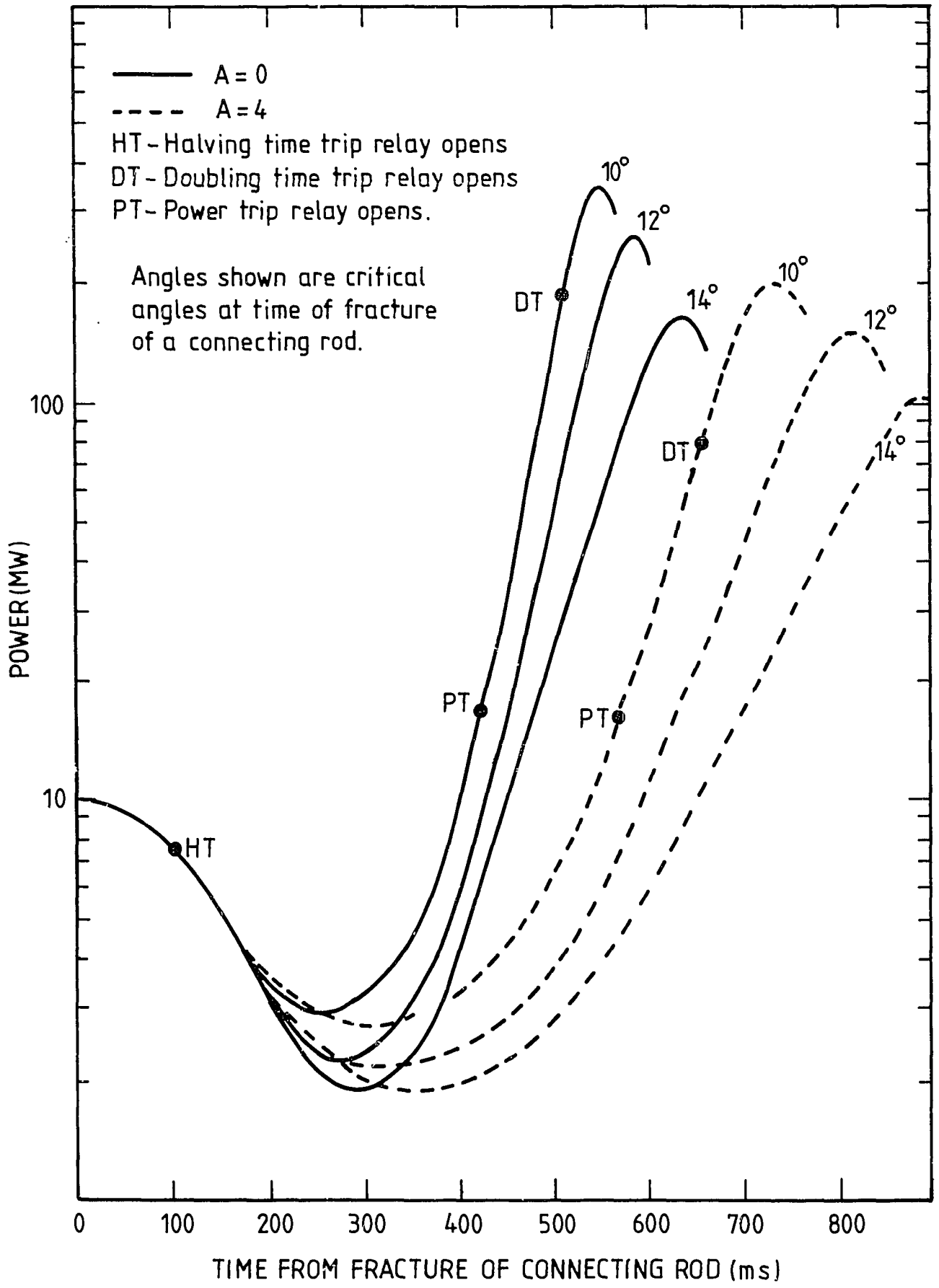

Figure 8 Calculated power transients following loss of a central CCA from 10°

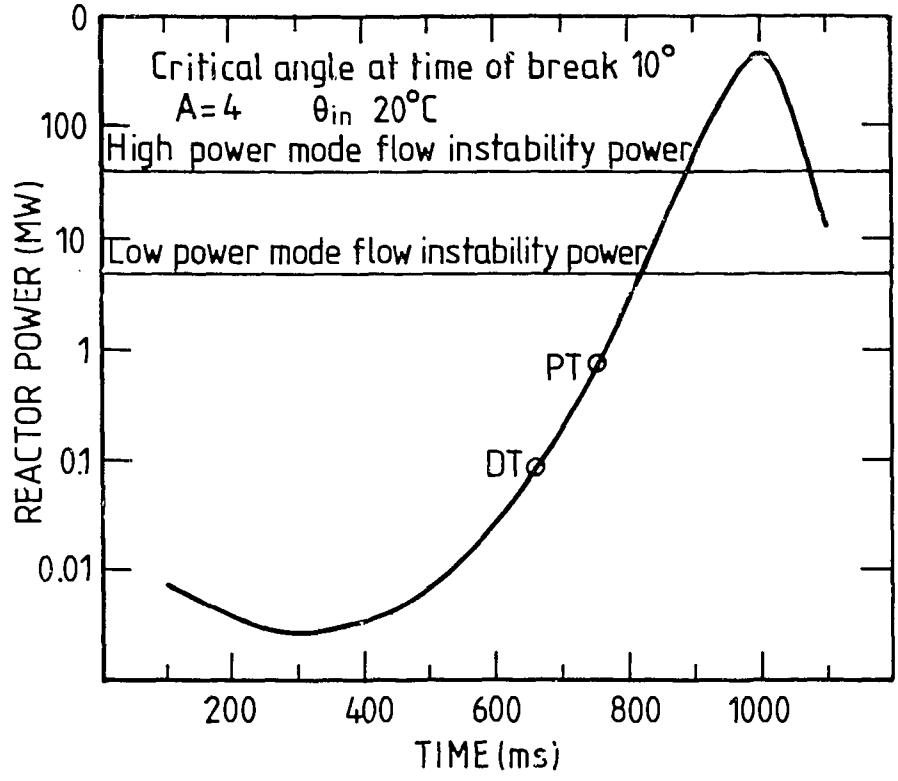

Figure 9 Times of trip relays opening for loss of arm accident from 10° and an initial power of 10 kW (low power mode)

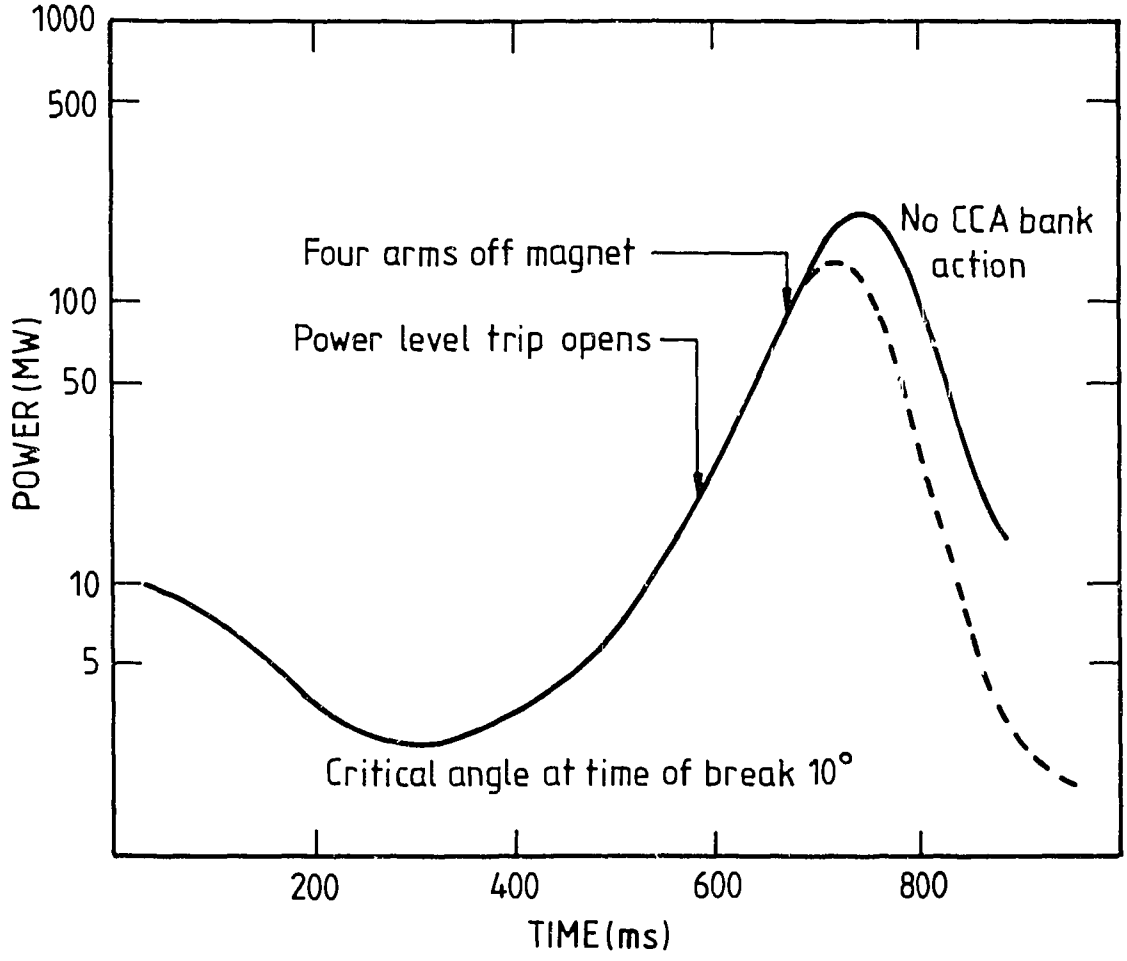

Figure 10 Calculated reactor power transient after loss of a central CCA with shutdown by four of the remaining arms starting 100 ms after the power level trip relay opens

APPENDIX A
DETERMINATION OF TRIP DELAY TIMES

A1. INTRODUCTION

This appendix sets out the procedures used to determine the delay time between initation of the loss-of-arm signal and trip relays opening for the HIFAR period and flux level trip units. A hybrid computer coupled to a voltage-to-current converter was used to drive the inputs to both units.

To confirm the testing procedure and equipment, the delay time was also determined for exponential signals which duplicated some of those used by Corran and Witt [1978]. The units were tested as received after routine maintenance.

The hardware attached to the hybrid computer had also been used by Corran and Witt. It included a cable plus a 1000 pF capacitor to simulate the greatest variation in cable capacitance to be expected in the actual HIFAR instrumentation.

The exponential function was generated at the analogue computer and its initiation was controlled from the digital computer with precise timing clocked by the analogue machine's time base.

The loss-of-arm function was obtained from ZAPP calculations over a range of time intervals fed from the digital computer to the analogue computer and converted to a suitable current before being used as input signals to the trip units. Timing was controlled in the same way as the exponential test signal.

A2. TEST PROCEDURES

(a) Read the appropriate function from the paper tape keyboard into the digital program FUNK-640. Set sense switch B to stop between function output sweeps.

(b) Adjust the analogue circuit parameters to the required setting.

(c) Reset period meter trips and ensure a steady infinite doubling time, or make sure that the flux level meter trip is not exceeded by the selected level.

(d) Press run-single-run buttons to sweep through the function once. Each time base will stop once a trip is caused. In the case of the exponential function, the current signal will also be halted at the trip level.

(e) The appropriate time base signals are then noted and the digital computer run-single-run buttons used to return to the initial settings.

(f) The analogue circuit parameters are incremented and steps (c) to (e) repeated for the desired range.

A3. TEST CONDITIONS

The doubling time trip setting was kept at 7s for all tests. No halving time trips were required for the exponential test signal and the doubling times, since the flux level trip unit did not vary with capacitative loading. Power sensitivity was 1 μA/MW for the period meter and 5.25 μA/MW for the flux level meter, this value being rounded to 5 μA/MW for ease of calculation and scaling.

A4. RESULTS - PERIOD METERS

A4.1 Loss-of-Arm Signal

Halving time trips occurred within 100 ms of signal initiation for both free fall and resisted arm motion for input currents greater than those corresponding to an initial power of 10 kW. For an initial power of 100 W, the delay time measured was 218 ms. Doubling time trips had a delay time of $\sim$ 650 ms in the case of resisted arm fall and $\sim$ 500 ms for free arm fall. These values did not change greatly over the range of initial currents nor with the input capacitative loading. Detailed results of these measurements are given in tables A1 and A2.

A4.2 Exponential Signal

Delay times were ~ 40 ms for a signal doubling time of 10 ms and rising to ~ 130 ms for a signal doubling time of 100 ms. No dependence on capacitative loading was shown. The results are listed in table A3.

A5. RESULTS - FLUX LEVEL METERS

A5.1 Loss-of-Arm Signal

Analysis of delay times showed that it took an almost constant 20-30 ms from the time for the input signal to pass the trip point and the trip relays to open. The detailed results for these measurements are given in tables A4 and A5. It will be noted from table A.4 that on one occasion no trip was recorded.

A5.2 Exponential Signal

Again, it took an almost constant 20-30 ms from the time taken by the input signal to pass the trip point and the relays to open. Detailed results are given in Table A6.

A6. REFERENCE

Corran, E.R., Witt, H. [1978] - AAEC unpublished report OD/HSA 33.

TABLE A1
RESULTS OF PERIOD METER MEASUREMENTS FOR
LOSS OF ARM FUNCTION WITH NORMAL MODERATOR LEVEL

INITIAL CURRENT (AMPS)	DOUBLING TRIP TIME (SECS)	HALVING TRIP TIME (SECS)	DOUBLING TRIP TIME (SECS)	HALVING TRIP TIME (SECS)
1.0E-10	0.715	0.218	0.760	NIL
2.0E-10	0.700	0.713	0.735	0.303
1.0E- 9	0.670	0.119	0.690	0.163
2.0E- 9	0.660	0.112	0.680	0.138
1.0E- 8	0.660	0.103	0.660	0.108
2.0E- 8	0.650	0.097	0.660	0.104
1.0E- 7	0.650	0.096	0.650	0.096
2.0E- 7	0.650	0.095	0.650	0.096
1.0E- 6	0.650	0.098	0.650	0.096
2.0E- 6	0.650	0.098	0.650	0.096
6.0E- 6	0.650	0.095	0.650	0.095
8.0E- 6	0.650	0.096	0.650	0.097
1.0E- 5	0.660	0.095	0.660	0.097
1.2E- 5	0.660	0.101	0.670	0.098
1.4E- 5	0.670	0.098	0.670	0.099
1.6E- 5	0.068	0.098	0.680	0.100
1.8E- 5	0.695	0.097	0.695	0.098
2.0E- 5	0.710	0.097	0.710	0.097

TABLE A2
RESULTS OF PERIOD METER MEASUREMENTS FOR
LOSS OF ARM FUNCTION WITH NO MODERATOR PRESENT

	C = 297 PF		C = 1292 PF	
INITIAL CURRENT (AMPS)	DOUBLING TRIP TIME (SECS)	HALVING TRIP TIME (SECS)	DOUBLING TRIP TIME (SECS)	HALVING TRIP TIME (SECS)
1.0E-10	0.537	0.219	0.560	NIL
2.0E-10	0.525	0.175	0.546	0.292
1.0E-09	0.510	0.125	0.517	0.159
2.0E-09	0.497	0.108	0.510	0.134
1.0E-08	0.484	0.096	0.501	0.111
2.0E-08	0.495	0.099	0.498	0.102
1.0E-07	0.487	0.095	0.485	0.094
2.0E-07	0.493	0.100	0.496	0.099
1.0E-06	0.494	0.097	0.489	0.094
2.0E-06	0.497	0.099	0.489	0.093
6.0E-06	0.500	0.097	0.498	0.098
8.0E-06	0.499	0.091	0.499	0.094
1.0E-05	0.513	0.096	0.515	0.099
1.2E-05	0.521	0.097	0.519	0.093
1.4E-05	0.531	0.095	0.526	0.094
1.6E-05	0.547	0.099	0.546	0.098
1.8E-05	0.557	0.093	0.554	0.096
2.0E-05	0.576	0.192	0.580	0.099

TABLE A3
RESULTS OF PERIOD METER MEASUREMENTS FOR
POSITIVE EXPONENTIAL FUNCTION (DOUBLING TIME ONLY)

DOUBLING TIME (SECS)	INITIAL CURRENT (AMPS)	C = 297 PF TRIP TIME (SECS)	C = 297 PF FINAL CURRENT (AMPS)	C = 1292 PF TRIP TIME (SECS)	C = 1292 PF FINAL CURRENT (AMPS)
0.01	1.0E- 8	0.039	0.143E- 6	0.042	1.15E- 7
	1.0E- 7	0.037	1.310E- 6	0.037	1.33E- 6
	1.0E- 6	0.036	1.210E- 5	0.036	1.22E- 5
	1.0E- 5	0.046	2.400E- 4	0.047	2.48E- 4
0.03	1.0E- 8	0.071	5.100E- 8	0.074	5.50E- 8
	1.0E- 7	0.069	4.800E- 7	0.069	4.80E- 7
	1.0E- 6	0.067	4.600E- 6	0.067	4.60E- 6
	1.0E- 5	0.070	4.900E- 5	0.070	4.90E- 5
0.10	1.0E- 8	0.140	2.600E- 8	0.143	2.68E- 8
	1.0E- 7	0.135	2.540E- 7	0.136	2.56E- 7
	1.0E- 6	0.133	2.490E- 6	0.132	2.49E- 6
	1.0E- 5	0.134	2.530E- 5	0.134	2.52E- 5

TABLE A4
RESULTS OF FLUX LEVEL TRIP METER MEASUREMENTS FOR
LOSS OF ARM FUNCTION WITH NORMAL MODERATOR LEVEL

TRIP SETTING (WATTS)	INITIAL CURRENT (AMPS)	TIME TO TRIP (SECS)	TRIP SETTING (WATTS)	INITIAL CURRENT (AMPS)	TIME TO TRIP (SECS)
1.5E+05	1.0E-07	0.750	1.1E+07	1.0E-05	0.670
	2.0E-07	0.710		2.0E-05	0.630
1.0E+06	1.0E-06	0.680		4.0E-05	0.590
	2.0E-06	0.640		5.0E-05	0.570
6.0E+06	2.0E-06	0.720	1.2E+07	1.0E-05	0.670
	1.0E-05	0.630		2.0E-05	0.640
	2.0E-05	0.590		4.0E-05	0.590
7.0E+06	2.0E-06	0.730		5.0E-05	0.580
	1.0E-05	0.640	1.3E+07	1.0E-05	0.675
	2.0E-05	0.600		2.0E-05	0.630
8.0E+06	2.0E-06	0.740		4.0E-05	0.590
	1.0E-05	0.650		5.0E-05	0.580
	2.0E-05	0.610	1.4E+07	1.0E-05	0.675
	4.0E-05	0.560		2.0E-05	0.640
9.0E+06	2.0E-06	0.750		4.0E-05	0.590
	1.0E-05	0.650		5.0E-05	0.590
	2.0E-05	0.610	1.5E+07	1.0E-05	0.680
	4.0E-05	0.570		2.0E-05	0.645
1.0E+07	2.0E-06	NO TRIP		4.0E-05	0.600
	1.0E-05	0.660		5.0E-05	0.590
	2.0E-05	0.620			
	4.0E-05	0.580			
	5.0E-05	0.560			

TABLE A5
RESULTS OF FLUX LEVEL TRIP METER MEASUREMENTS FOR
LOSS OF ARM FUNCTION WITH NO MODERATOR

TRIP SETTING (WATTS)	INITIAL CURRENT (AMPS)	TIME TO TRIP (SECS)	TRIP SETTING (WATTS)	INITIAL CURRENT (AMPS)	TIME TO TRIP (SECS)
1.5E+05	1.0E-07	0.551	1.1E+07	2.0E-06	0.584
	2.0E-07	0.526		1.0E-05	0.491
1.0E+06	2.0E-07	0.579		2.0E-05	0.462
	1.0E-06	0.506		4.0E-05	0.437
	2.0E-06	0.479		5.0E-05	0.426
6.0E+06	1.0E-06	0.586	1.2E+07	2.0E-06	0.590
	2.0E-06	0.543		1.0E-05	0.491
	1.0E-05	0.470		2.0E-05	0.468
7.0E+06	1.0E-06	0.604		4.0E-05	0.442
	2.0E-06	0.548		5.0E-05	0.438
	1.0E-05	0.475	1.3E+07	2.0E-06	0.597
8.0E+06	2.0E-06	0.562		1.0E-05	0.496
	1.0E-05	0.484		2.0E-05	0.471
	2.0E-05	0.456		4.0E-05	0.446
	4.0E-05	0.430		5.0E-05	0.433
9.0E+06	2.0E-06	0.563	1.4E+07	2.0E-06	0.603
	1.0E-05	0.581		1.0E-05	0.495
	2.0E-05	0.463		2.0E-05	0.480
	4.0E-05	0.432		4.0E-05	0.449
1.0E+07	2.0E-06	0.569		5.0E-05	0.445
	1.0E-05	0.490	1.5E+07	1.0E-05	0.507
	2.0E-05	0.467		2.0E-05	0.474
	4.0E-05	0.432		4.0E-05	0.454
	5.0E-05	0.425		5.0E-05	0.447

TABLE A6
RESULTS OF FLUX LEVEL TRIP METER MEASUREMENTS FOR
POSITIVE EXPONENTIAL FUNCTION

INITIAL CURRENT (AMPS)	TRIP SETTING (WATTS)	0.01 SEC DOUBLING EXP. TIME (SECS)	0.03 SEC DOUBLING EXP. TIME (SECS)	0.10 SEC DOUBLING EXP. TIME (SECS)
5.0E-08	1.5E+05	0.096	0.203	0.516
5.0E-08	1.0E+06	0.103	0.241	0.657
5.0E-06	6.0E+06	0.052	0.104	0.287
5.0E-06	7.0E+06	0.054	0.112	0.311
5.0E-06	8.0E+06	0.056	0.117	0.331
5.0E-06	9.0E+06	0.057	0.121	0.346
5.0E-06	1.0E+07	0.059	0.126	0.362
5.0E-06	1.1E+07	0.060	0.130	0.375
5.0E-06	1.2E+07	0.061	0.134	0.390
5.0E-06	1.3E+07	0.062	0.138	0.402
5.0E-06	1.4E+07	0.063	0.140	0.410
5.0E-06	1.5E+07	0.064	0.143	0.421

APPENDIX B
THE VOIDING MODEL USED IN ZAPP

B1. INTRODUCTION

For fast transients in water-cooled reactors, the generation of steam voids can be an important reactivity feedback mechanism, because of the magnitude and the extremely rapid introduction of the associated negative reactivity.

In principle, thermohydraulic theory should enable the growth of steam voids to be calculated, but in practice a rather arbitrary choice of constants must be made to derive numerical results. Testing against experiment must then be used as a guide to such selection.

The code ZAPP has no provision to enable thermohydraulic calculations to be made. Nucleate boiling is modelled by forcing the code to produce a rapidly increasing 'boiling' boundary layer at the fuel coolant interface once saturation temperature is reached. It was tempting therefore to couple this increasing boundary layer with a decrease in density with temperature. The parameters necessary to do this were the temperature of the boundary layer at which steam voids commenced to grow and the subsequent rate of decrease of density of the boundary layer with temperature. These constants were determined by 'best fitting' to data from the SPERT II BD22/24 transient experiments.

B2. COMPARISON OF RESULTS OBTAINED WITH THE MODEL AND EXPERIMENT

The first comparison was made by calculating the range of transients performed with the SPERT I core D12/25 with and without the voiding model. Spano and Miller [1962] subjected this core to increasingly severe transients which culminated in its destruction by a steam explosion. The experimentally observed energy releases at the time of peak power as a function of initial inverse power period and their ZAPP calculations are shown in figure B1. The void model gives good agreement with the observed values.

The second comparison is with the data of Singer [1967] who determined the development of the void fraction in an electrically heated channel rather similar to the concentric HIFAR coolant channels. The heater in the channel was subjected to a square wave power input whose duration was 100 ms and the adiabatic temperature rise rate was used as a parameter in the analysis. In a reactor transient, the power is not constant, but if the adiabatic temperature rise rate is calculated at the time of peak power, it bears a rough resemblance to the conditions of Singer's experiments. The comparison between Singer's data and HIFAR calculation for an initial reactor period of 50 ms is shown in figure B2. If the HIFAR void fraction is scaled by the ratio of the adiabatic temperature rise rate of the Singer data to that of the HIFAR calculations at the time of peak power, reasonable agreement is shown between the two estimates of void growth.

B3. CONCLUSION

It is considered that the void model used in the loss-of-arm accident analysis gives reasonable estimates of the contribution of voids to shutdown.

B4. REFERENCES

Singer, R.M. [1967] - ANL 7337.

Spano, A.H., Miller, R.W., [1962] - IDO-16790.

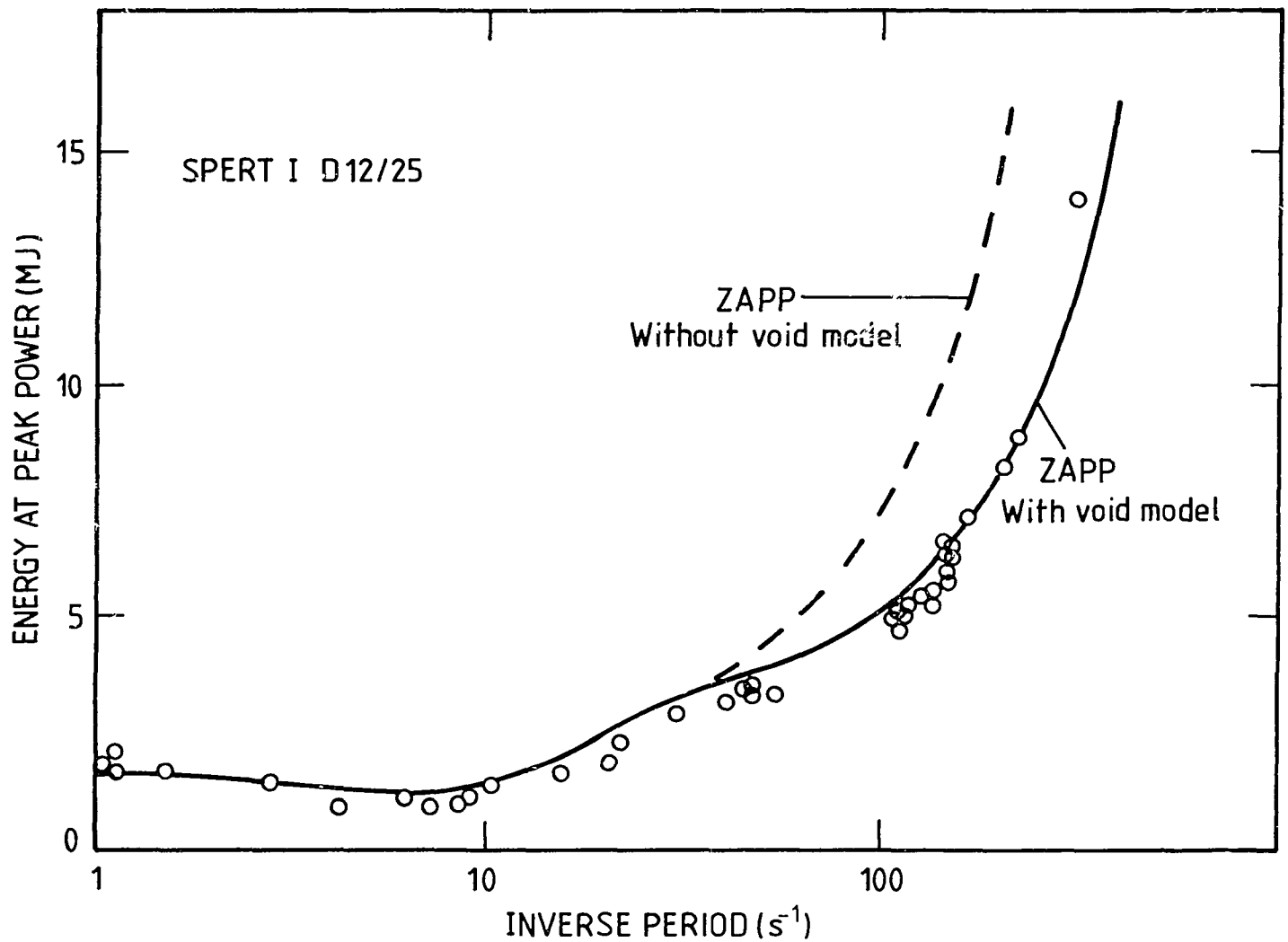

Figure B1 Comparison of ZAPP calculations with energy release data from SPERT D12/25 core

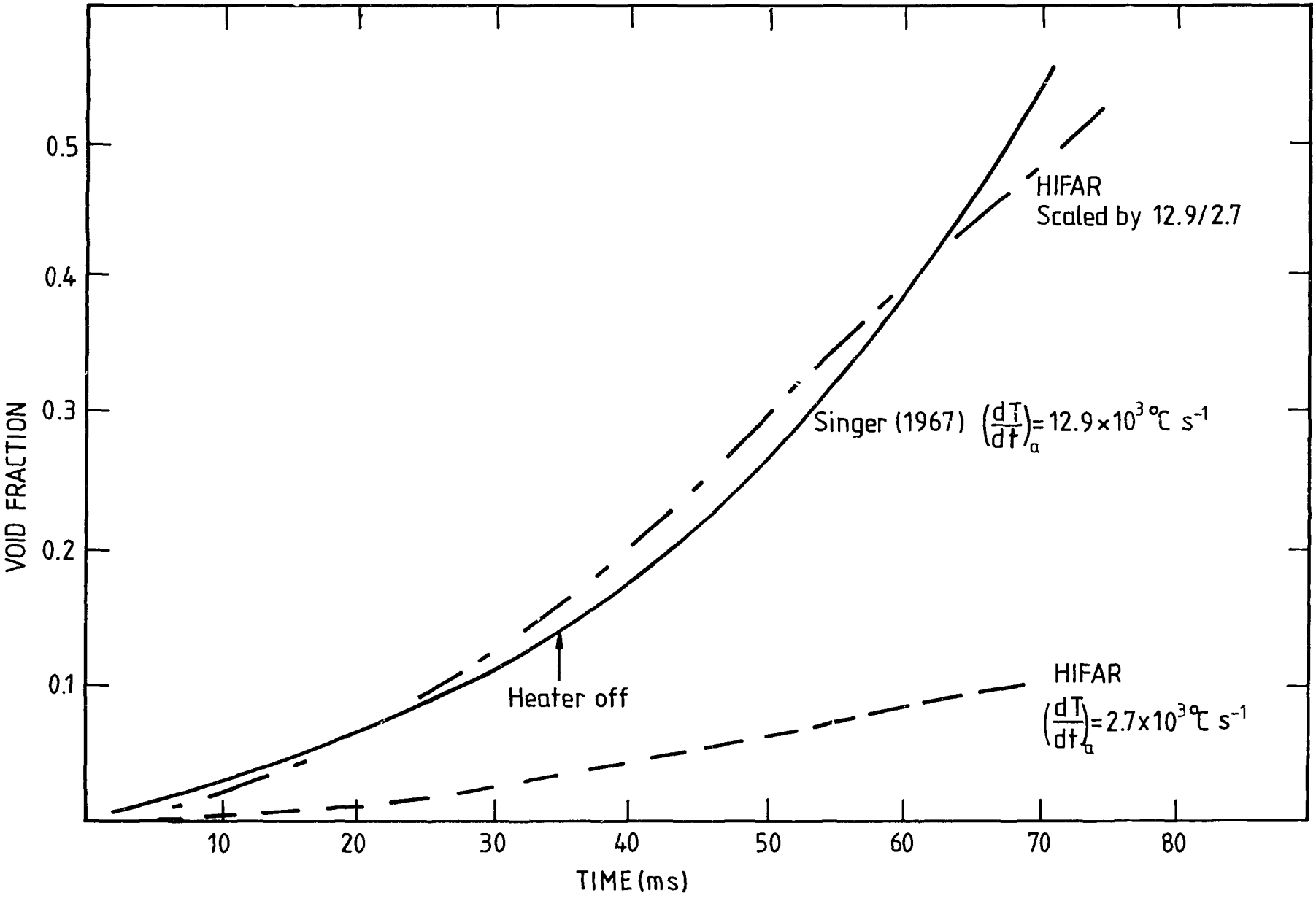

Figure B2 Comparison of ZAPP HIFAR void growth calculations with Argonne National Laboratory void growth measurements